Real-Time Walk Detection for Robotic Hip Exoskeleton Applications

Hang Man Cho¹, Inseung Kang^{1,2}, Dongho Park^{1,3}, Dean D. Molinaro^{1,3}, and Aaron J. Young^{1,3}

Abstract—Detection of the user's walking is a critical part of exoskeleton technology for the full automation of smooth and seamless assistance during movement transitions. Researchers have taken several approaches in developing a walk detection system by using different kinds of sensors; however, only a few solutions currently exist which can detect these transitions using only the sensors embedded on a robotic hip exoskeleton (i.e., hip encoders and a trunk IMU), which is a critical consideration for implementing these systems in-the-loop of a hip exoskeleton controller. As a solution, we explored and developed two walk detection models that implemented a finite state machine as the models switched between walking and standing states using two transition conditions: stand-to-walk and walk-to-stand. One of our models dynamically detected the user's gait cycle using two hip encoders and an IMU; the other model only used the two hip encoders. Our models were developed using a publicly available dataset and were validated online using a wearable sensor suite that contains sensors commonly embedded on robotic hip exoskeletons. The two models were then compared with a foot contact estimation method, which served as a baseline for evaluating our models. The results of our online experiments validated the performance of our models, resulting in 274 ms and 507 ms delay time when using the HIP+IMU and HIP ONLY model, respectively. Therefore, the walk detection models established in our study achieve reliable performance under multiple locomotive contexts without the need for manual tuning or sensors additional to those commonly implemented on robotic hip exoskeletons.

Index Terms— Robotic Hip Exoskeleton, Walk Detection, Locomotion, Wearable Sensor

I. INTRODUCTION

Previously, researchers have taken different approaches in developing a walk detection system for lower-limb assistive devices. In our daily lives, we commonly walk over short bouts with frequent short rests [1]. A walk detection system could easily automate the switch of assistance of these assistive devices in our daily lives and even help provide a smooth transition of assistance between standing and walking. One common method is using bio-electrical sensors, such as electromyography (EMG) signals [2]–[8]. While this approach is efficient in detecting the user's movement prior to any visible kinematic changes, bio-electrical signals are often unreliable and hard to calibrate compared to signals

from onboard mechanical sensors [9]. To overcome the unreliability of bio-electrical signals, other researchers installed Force Sensing Resistors (FSRs) into the shoe to directly detect a gait event such as toe-off or heel-strike [10]–[13]. This approach, however, is only ideal for devices that assist distal joints where the sensor could easily be located (e.g., under the user's foot), and FSRs tend to wear out easily from multiple usages.

An Inertial Measurement Unit (IMU) is another mechanical sensor that has been widely used for walk detection. Atalante (Wandercraft, France), a self-balancing lower-limb exoskeleton, employed a machine learning-based user intent detector using an upper-body IMU [14]. Brescianini et al. used an IMU sensor and FSR mounted hand crutch for motion detection when using an exoskeleton [15]. Ding et al. developed a portable system using an IMU placed on the user's shoe for detecting different gait events [16]. While all these methods are promising, these methods are nonideal when integrating into a hip exoskeleton system as the sensors are often required to be positioned at a distal location. Additionally, the majority of these methods require additional sensors to be utilized with manual tuning procedures, which greatly hinders deployment to a commercially available system. Several researches on hip exoskeletons have shown that hip exoskeletons are capable of providing meaningful assistance to able-bodied and clinical populations by saving their metabolic cost or augmenting their strength [17]–[21]. However, there hasn't been enough research on a walk detection system for hip exoskeletons that could provide reliable and robust performance.

For the reliable performance of a walk detection system, it is critical to utilize native sensors on the device. For hip exoskeletons, such as the Gait Enhancing and Motivating System (GEMS) developed by Samsung Electronics [22]-[24], a conventional sensor suite includes two joint encoders for the hip joint position and velocity bilaterally and a trunk IMU for the acceleration and gyroscope data. Previously for these types of exoskeletons (e.g., GEMS), a walk detector algorithm was developed by estimating the user's foot contact using the trunk IMU with a predetermined threshold [22]. While this simple method shows decent performance for detecting the user's intent, its robustness in other locomotor contexts, such as varying acceleration, is questionable. Furthermore, setting a static threshold for detecting the user's movement may only be applicable in a laboratory setting where the user's limb motion is highly constrained before walking.

The main objective of this study was to develop and validate a novel, real-time user-independent walk detector

^{*}This work was supported in part by the NSF NRI Award #1830215 and the NSF GRFP Award #DGE-1650044.

¹ H. M. Cho, I. Kang, D. Park, D. D. Molinaro, and A. J. Young are with the School of Mechanical Engineering, Georgia Institute of Technology, Atlanta, GA, 30332 USA. (corresponding author: Hang Man Cho)

²I. Kang is with the Department of Brain and Cognitive Sciences, Massachusetts Institute of Technology, Cambridge, MA, 02139 USA.

³D. Park, D. D. Molinaro and A. J. Young are with the Institute for Robotics and Intelligent Machines, Georgia Institute of Technology, Atlanta, GA, 30332 USA.

that is robust in various acceleration and deceleration settings and accommodates natural user postures during standing. To quantitatively evaluate the effect of different sensors on the model, two different detectors were designed using: 1) two hip encoders (referred to as HIP ONLY) and 2) two hip encoders and an IMU (referred to as HIP+IMU). The performance of these detectors were compared with existing method such as foot contact estimation method (referred to as IMU ONLY) [22]. The central hypothesis for our study is that the HIP+IMU model will further improve the overall performance of the walk detector because using multiple sensors could make the detector less vulnerable to outlying situations. The key contribution of our study is that the algorithm is easily deployable to other wearable systems without the need for manual tuning and requires a minimal number of sensors to robustly detect the user's movement in various locomotion contexts.

II. METHODS

A. Offline Model Development

Our models were initially developed offline, using an open-source dataset [25], and their performance were validated on a wide range of subjects. The dataset included 22 able-bodied subjects ambulating across five different locomotion modes (level-ground, ramp ascent/descent, and stair ascent/descent). Each model implemented a finite state machine that switched between walking and standing states

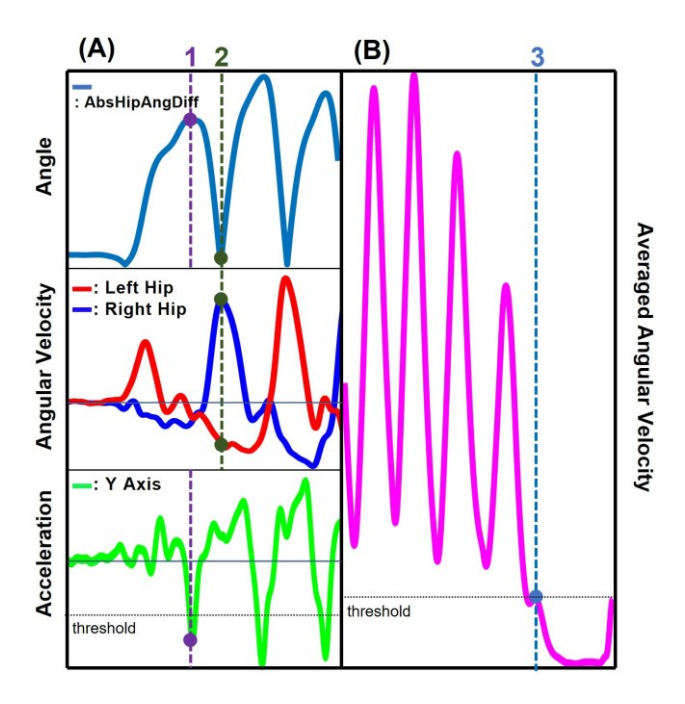


Fig. 1. (A) Three time series plots of HIP+IMU model during stand-to-walk transition (B) A time series plot of HIP+IMU model during walk-to-stand transition. The purple dashed vertical line (1) represents the maximum hip angle, where the trunk acceleration along the Y axis (vertical axis) is already below the threshold. The green dashed vertical line (2) represents hip crossing, where the angular velocity of the left and right hip have opposite signs. The blue dashed vertical line (3) represents the transition to standing state as the angular velocity drops below the threshold.

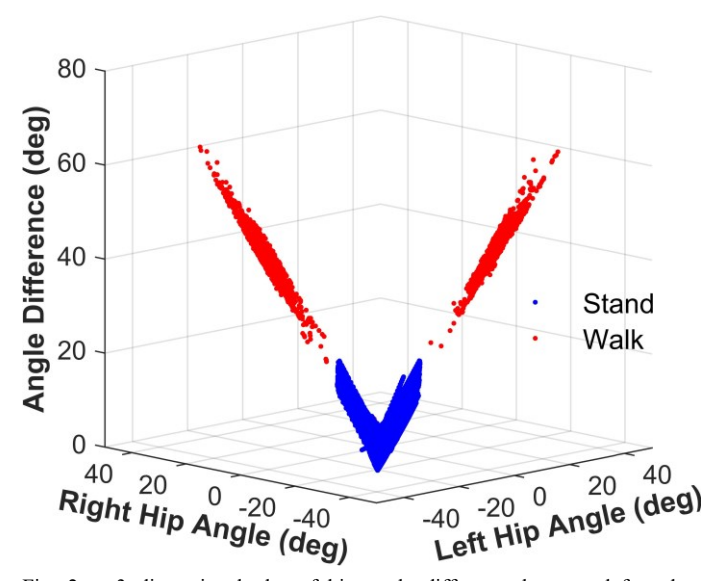


Fig. 2. 3 dimensional plot of hip angle difference between left and right hip joint during heel-strike. The plot illustrates a clear boundary between standing state and walking state at 15 degrees, which became the predetermined threshold for the HIP ONLY [22].

using 2 transition conditions: stand-to-walk and walk-to-stand.

After the initial offline development, we designed two novel walk detector models: HIP+IMU model and HIP ONLY model. The stand-to-walk transition condition for HIP+IMU model used two hip encoders, one on each hip joint, and a trunk-mounted IMU. This transition condition focused on detecting the user's initial heel-strike and the following hip joint crossing (Fig. 1). The first heel-strike was detected by the conjunction of a maximum in hip angle difference and a corresponding vertical acceleration from the trunk IMU below a predefined threshold. The HIP+IMU model went through the transition if the following hip crossing was detected within 800 ms after the first heal-strike. The hip crossing will be identified by minimum hip angle difference that is around zero along with the opposite signs for left and right hip angular velocity.

The stand-to-walk transition condition for the HIP ONLY model used two hip encoders. The transition condition is similar to the HIP+IMU model. Instead, the model detected the heel-strike if a maximum hip angle difference is above 15 degrees without using pelvis acceleration data (Fig. 2). The walk-to-stand transition condition was identical for both the HIP+IMU model and HIP ONLY model. Instead of detecting the angle between hip joints, the walk-to-stand transition condition only used hip angular velocity data. This was due to the nature of standing state being in various postures, unlike the walking state which has its own unique motion. The angular velocity data was filtered using a moving average filter. The window size of a moving average filter was determined to be 250 ms which provided a proper balance between a delay time and an amplitude of oscillation (Fig. 3). As soon as the average angular velocity between the two hip joints crosses the threshold, our model detected the walk-

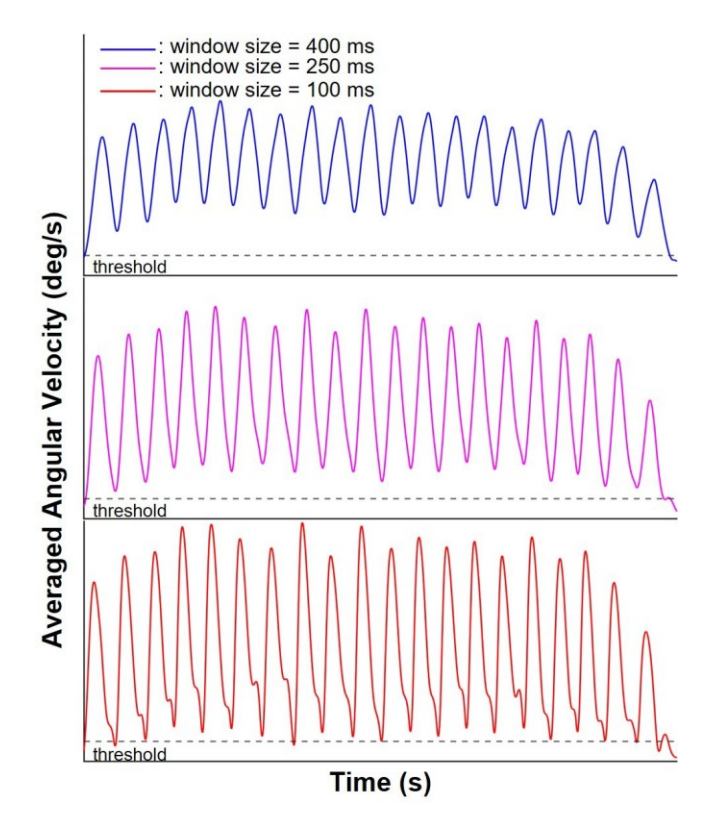


Fig. 3. Time series plot of hip angular velocity filtered with different window sizes of moving average filter. The red line, with a window size of 100 ms, consistently crosses the threshold during steady-state walking. The blue line, with a window size of 400ms, has the largest delay time which could negatively affect the overall performance.

to-stand transition.

B. Real-time Wearable Sensor Suite

Our real-time wearable sensor suite was developed to validate our pre-designed models in various acceleration/deceleration settings in real-time (Fig. 4). Additionally, the sensor suite was used to verify whether several parameters from the offline model development were applicable during online validation. The sensor suite consisted of two electro-goniometers (PASPORT Goniometer Probe, PASCO Scientific) and an IMU (MPU 9250, InvenSense) mounted on the trunk. The two goniometers were mounted on each hip joint with hip and waist straps, and the IMU was integrated into our custom-made PCB that is mounted in an electronic backpack. Each LED on the PCB lit up when walking was detected for each walk detector model. The switch was used for simple static calibration to zero the data during the standing state.

C. Online Human Subject Validation

We recruited four able-bodied subjects with an average age of 23.25 ± 4.27 years, a height of 174.31 ± 6.25 cm, and a body mass of 66.02 ± 14.05 kg to online validate our model in real-time. The study was approved by the Georgia Institute of Technology Institutional Review Board and informed written consent was obtained for all

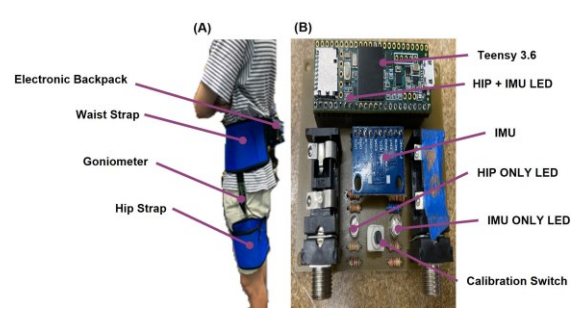


Fig. 4. (A) Real-time wearable sensor suite for online human subject validation (B) The custom-made main circuit board houses the connector for two electro-goniometers and the trunk mounted IMU.

subjects. Subjects were asked to wear the sensor suite and walk on a treadmill (Bertec, Columbus) in four different acceleration/deceleration settings (0.2, 0.4, 0.6, 0.8 m/s²) and five incline settings (level-ground, ramp ascent/descent at 5° and 10°). The sensor suite was synchronized with the treadmill using TCP/IP communication. There were three trials for each acceleration/deceleration and incline/decline setting. The speed of the treadmill was accelerated up to 1.2 m/s from 0 m/s, maintained 1.2 m/s for five seconds, and then decelerated back to 0 m/s. For every trial, the subject's motion was not constrained before walking. As the subject walked on the treadmill, the mean and standard deviation of the delay time for our two walk detector models and the foot contact estimation method (as the baseline) using the trunk IMU (referred to as IMU ONLY) [22] were validated and compared. The delay time of our two models for the standto-walk transition was measured from the first hip crossing, which took place after the first heel-strike detection (Fig. 5), to the actual time the models detected the transition. The delay time of IMU ONLY model was measured from the time the treadmill started running to the actual time when the transition was detected in the model. The delay time of all three models for the walk-to-stand transition was measured from the actual time the models detected the transition to the time when the speed of the treadmill returned back to zero after deceleration.

III. RESULTS

Overall delay time for the stand-to-walk transition of HIP+IMU model remained highly consistent across all the different settings with an average delay time of 274 ms. The stand-to-walk transition of HIP ONLY model also remained consistent with a similar average delay time except for a few settings. For instance, the mean delay time for trials with 0.2 m/s² of acceleration at 10° decline was 2015 ms. For IMU ONLY model, its average delay time was 1115.7 ms. Also, its delay time had tendency to increase with slower acceleration and higher incline settings. Unlike HIP+IMU model and HIP ONLY model, the delay time of IMU ONLY model for the stand-to-walk transition was much less consistent, leading to an average standard deviation of around 440 ms for each setting.

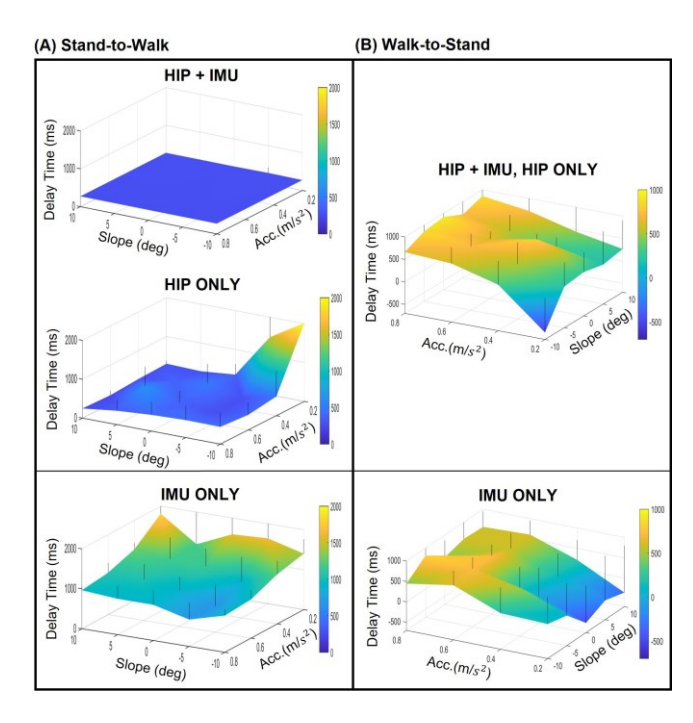


Fig. 5. (A) Surface plot showing the delay time for stand-to-walk transition (B) Surface plot showing the delay time for walk-to-stand transitions with respect to different acceleration/deceleration and incline/decline settings. Black vertical lines on the surface along the z-axis show the value of standard deviations for each setting. A negative slope means that the subject went through decline trials corresponding to that angle.

During the walk-to-stand transition, HIP+IMU model and HIP ONLY model had an average delay time of 498.7 ms, which was a higher delay time than their delay time for the stand-to-walk transition. For IMU ONLY model, compared to its delay time for stand-to-walk transition, it was notable that the average delay time was 313.3 ms.

For HIP+IMU model and HIP ONLY model, the false positive rate was zero during the steady-state. IMU ONLY model also had almost zero false positive rate (0.26%) during steady-state. All the methods accurately detected the walking state during steady-state walking at 1.2 *m/s* without unintentionally going through the walk-to-stand transition.

IV. DISCUSSION

The key contribution of our study is that the algorithm is easily deployable to other wearable systems without a need for manual tuning and requires a small number of sensors to robustly detect the user's movement for standing and walking. Overall, our models were able to detect walking during steady-state with an accuracy of 100%. Furthermore, our models proved that using hip encoders for detecting stand-to-walk transition is highly recommended. Not only did our two models outperform IMU ONLY model with a shorter delay time, but they also had better consistency overall in acceleration/deceleration and incline/decline settings. In comparing HIP+IMU model and HIP ONLY model, both models had similar performance in most of the settings. This similarity might potentially make HIP ONLY model a preferable option as it utilized fewer numbers of sensors.

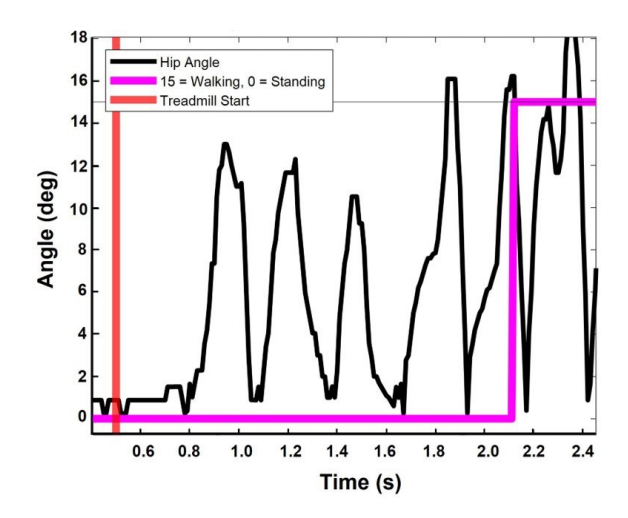


Fig. 6. The time series plot of HIP ONLY model during one of $0.2 \, m/s^2$ deceleration and 10° decline trials. The first three maximum hip angles did not cross the threshold, causing a much longer delay time for this method for $0.2 \, m/s^2$ deceleration and 10° decline.

However, some trials with 0.2 and 0.4 m/s^2 , and 10° decline settings revealed some drawbacks of setting a simple angle threshold for stand-to-walk detection. During ramp descent walking, subjects tended to show less peak hip angle, making it harder to cross our predetermined threshold (Fig. 6). In this case, lowering the threshold could be a possible solution. However, lowering the angle threshold would more likely cause false peak detection. With a lower threshold, subjects would much more likely to stand with a hip angle that is already larger than the threshold, causing our model to detect stand-to-walk transition even when the subject is simply standing. HIP+IMU model would prevent the above problems because the IMU threshold for this model won't be triggered when the subject is simply in standing state. In other words, HIP+IMU model as their data would more accurately detect heel-strike using maximum hip angle data along with trunk vertical acceleration data.

For walk-to-stand transition, it should be mentioned that, for trials with higher deceleration, subjects are more likely to take one more step after the treadmill stopped. Since the delay time was measured with respect to the time when the treadmill stopped, this extra step caused a much higher delay time for trials with higher deceleration settings. Also, the performance of our models during lower deceleration is worth noting. The average delay time for trials with 0.2 m/s^2 deceleration at the level ground was only 273 ms. This brings upon the potential for its outstanding performance even for people with limited mobility like stroke patients, whom typically walk at a slower pace. For IMU ONLY model, the average delay time for the same setting was -461 ms. While a lower value of delay time generally leads to better performance, detection of walk-to-stand transition much before the actual transition might cause the device to stop its assistance in real-world scenarios regardless of the user's intent to stop walking.

One limitation of the study is that the delay time for

our models (HIP+IMU and HIP ONLY) and foot contact estimation method (IMU ONLY) had different starting points for stand-to-walk transition. Despite the seemingly higher delay time for IMU ONLY model across all settings, there were some trials in which IMU ONLY model had a shorter delay in real-time. Another limitation is that our model performed poorly during walk-to-stand transition for 0.2 m/s^2 deceleration and 10° decline trials with an average delay time of -353 ms. This limitation brings upon our future goal to integrate hip encoder and IMU in our model for walk-to-stand transitions. Also, our model should be tested on more subjects among various ranges of heights, weights, and ages for more accurate validation. The last limitation that should be noted is that the models were only tested on a single sensor suite, not an actuated device. This brings upon a possibility that our model could perform differently on a robotic hip exoskeleton where sensor signals are affected by actuation.

V. CONCLUSION

Our model based on a finite state machine proved that integrating hip encoders with an IMU effectively detects stand-to-walk and walk-to-stand transitions. Also, our model showed promising performance in being easily deployable to other wearable systems without a need for manual tuning and in requiring a menial number of sensors to robustly detect the user's movement in various locomotion contexts. Our results reveal that our model developed exoskeleton technology into more realistic settings where the users have much robust detection of walking in various settings and have fewer constraints in movement before walking. Future goals for this study include integrating our model with a robotic hip exoskeleton to test the performance of our models in the device and possibly applying this model for people with limited mobility.

REFERENCES

- [1] G. Klute, A. Segal, G. Bernatz, and M. Orendurff, "How humans walk: bout duration, steps per bout, and rest duration," *J Rehabil Res Dev*, vol. 45, pp. 1077–1989, 2008.
- [2] J. Okamura, "Emg-based prototype powered assistive system for walking aid," in *Proceedings of Asian Symposium on Industrial Automation* and Robotics, 1999, pp. 229–234, 1999.
- [3] S. Lee and Y. Sankai, "Power assist control for walking aid with hal-3 based on emg and impedance adjustment around knee joint," in IEEE/RSJ international conference on intelligent robots and systems, vol. 2, pp. 1499–1504, IEEE, 2002.
- [4] T. Nakai, "Development of power assistive leg for walking aid using emg and linux," *Proc. of ASIAR2001*, pp. 295–299, 2001.
- [5] J. Lobo-Prat, A. Q. Keemink, A. H. Stienen, A. C. Schouten, P. H. Veltink, and B. F. Koopman, "Evaluation of emg, force and joystick as control interfaces for active arm supports," *Journal of neuroengineering and rehabilitation*, vol. 11, no. 1, pp. 1–13, 2014.
- [6] D. Xu, X. Liu, and Q. Wang, "Knee exoskeleton assistive torque control based on real-time gait event detection," *IEEE Transactions* on Medical Robotics and Bionics, vol. 1, no. 3, pp. 158–168, 2019.
- [7] A. L. Benabid, T. Costecalde, A. Eliseyev, G. Charvet, A. Verney, S. Karakas, M. Foerster, A. Lambert, B. Morinie're, N. Abroug, et al., "An exoskeleton controlled by an epidural wireless brain-machine interface in a tetraplegic patient: a proof-of-concept demonstration," The Lancet Neurology, vol. 18, no. 12, pp. 1112–1122, 2019.
- [8] F. Astudillo, J. Charry, I. Minchala, and S. Wong, "Lower limbs motion intention detection by using pattern recognition," in 2018 IEEE Third Ecuador Technical Chapters Meeting (ETCM), pp. 1–6, IEEE, 2018.

- [9] P. Artemiadis and M. Ison, "The role of muscle synergies in myoelectric control: Trends and challenges for simultaneous multifunction control," *Journal of Neural Engineering*, vol. 11, p. 051001, 2014.
- [10] Q. Guo and D. Jiang, "Method for walking gait identification in a lower extremity exoskeleton based on c4. 5 decision tree algorithm," *International Journal of Advanced Robotic Systems*, vol. 12, no. 4, p. 30, 2015.
- [11] A. Tsukahara, R. Kawanishi, Y. Hasegawa, and Y. Sankai, "Sit-to-stand and stand-to-sit transfer support for complete paraplegic patients with robot suit hal," *Advanced robotics*, vol. 24, no. 11, pp. 1615–1638, 2010.
- [12] J. S. Park, C. M. Lee, S.-M. Koo, and C. H. Kim, "Gait phase detection using force sensing resistors," *IEEE Sensors Journal*, vol. 20, no. 12, pp. 6516–6523, 2020.
- [13] C. Zhang, X. Zang, Z. Leng, H. Yu, J. Zhao, and Y. Zhu, "Human—machine force interaction design and control for the hit load-carrying exoskeleton," *Advances in Mechanical Engineering*, vol. 8, no. 4, p. 1687814016645068, 2016.
- [14] O. M. Alaoui, F. Expert, G. Morel, and N. Jarrasse', "Using generic upper-body movement strategies in a free walking setting to detect gait initiation intention in a lower-limb exoskeleton," *IEEE Transactions* on Medical Robotics and Bionics, vol. 2, no. 2, pp. 236–247, 2020.
- [15] D. Brescianini, J.-Y. Jung, I.-H. Jang, H. S. Park, and R. Riener, "Ins/ekf-based stride length, height and direction intent detection for walking assistance robots," in 2011 IEEE International Conference on Rehabilitation Robotics, pp. 1–5, IEEE, 2011.
- [16] S. Ding, X. Ouyang, T. Liu, Z. Li, and H. Yang, "Gait event detection of a lower extremity exoskeleton robot by an intelligent imu," *IEEE Sensors Journal*, vol. 18, no. 23, pp. 9728–9735, 2018.
- [17] G. S. Sawicki, O. N. Beck, I. Kang, and A. J. Young, "The exoskeleton expansion: improving walking and running economy," *Journal of NeuroEngineering and Rehabilitation*, vol. 17, no. 1, pp. 1–9, 2020.
- [18] K. Seo, J. Lee, Y. Lee, T. Ha, and Y. Shim, "Fully autonomous hip exoskeleton saves metabolic cost of walking," in 2016 IEEE International Conference on Robotics and Automation (ICRA), pp. 4628– 4635, 2016.
- [19] Y.-H. Kim, H.-J. Lee, S.-H. Lee, K. Seo, M. Lee, W. H. Chang, B.-O. Choi, and G.-H. Ryu, "Training for walking efficiency with a wearable hip-assist robot in patients with stroke: A pilot randomized controlled trial," vol. 50, pp. 3545–3552, 2019.
- [20] I. Kang, H. Hsu, and A. Young, "The effect of hip assistance levels on human energetic cost using robotic hip exoskeletons," *IEEE Robotics* and Automation Letters, vol. 4, no. 2, pp. 430–437, 2019.
- [21] P. W. Franks, G. M. Bryan, R. M. Martin, R. Reyes, A. C. Lakmazaheri, and S. H. Collins, "Comparing optimized exoskeleton assistance of the hip, knee, and ankle in single and multi-joint configurations," *Wearable Technologies*, vol. 2, 2021.
- [22] J. Jang, K. Kim, J. Lee, B. Lim, and Y. Shim, "Online gait task recognition algorithm for hip exoskeleton," in 2015 IEEE/RSJ International Conference on Intelligent Robots and Systems (IROS), pp. 5327–5332, IEEE, 2015.
- [23] J. Jang, J. Lee, B. Lim, and Y. Shim, "Natural gait event-based level walking assistance with a robotic hip exoskeleton," in 2018 40th Annual International Conference of the IEEE Engineering in Medicine and Biology Society (EMBC), pp. 1–5, IEEE, 2018.
- [24] D.-S. Kim, H.-J. Lee, S.-H. Lee, W. H. Chang, J. Jang, B.-O. Choi, G.-H. Ryu, and Y.-H. Kim, "A wearable hip-assist robot reduces the cardiopulmonary metabolic energy expenditure during stair ascent in elderly adults: a pilot cross-sectional study," *BMC geriatrics*, vol. 18, no. 1, pp. 1–8, 2018.
- [25] J. Camargo, A. Ramanathan, W. Flanagan, and A. Young, "A comprehensive, open-source dataset of lower limb biomechanics in multiple conditions of stairs, ramps, and level-ground ambulation and transitions," *Journal of Biomechanics*, vol. 119, p. 110320, 2021.